Applied Energy 313 (2022) 118856

Contents lists available at ScienceDirect

Applied Energy

journal homepage: www.elsevier.com/locate/apenergy

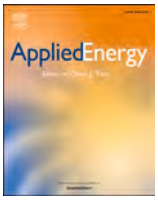

Optimal Port Microgrid Scheduling Incorporating Onshore Power Supply and Berth Allocation Under Uncertainty

Yue Zhang [a], Chengji Liang [a,c], Jian Shi [b,*], Gino Lim [c], Yiwei Wu [c]

[a] Institutes of Logistics Science and Technology, Shanghai Maritime University, PR China
[b] Department of Engineering Technology, University of Houston, United States
[c] Department of Industrial Engineering, University of Houston, United States

HIGHLIGHTS

- Seeks synergy between onshore power supply and microgrid for port electrification.
- Expand the conventional scheduling paradigm of port operation.
- Develops a two-stage method to co-optimize seaside operation and port energy management.
- Reveals the environmental and economic advantages of the joint scheduling approach.

ARTICLE INFO

Keywords:
Maritime transportation
Transportation Electrification
Onshore power supply
Port energy system
Microgrid

ABSTRACT

The high environmental impacts of maritime transportation have led to an increasing interest in adopting electricity as the ideal energy source within the sector. In this paper, we propose a novel integrated day-ahead scheduling algorithm to jointly optimize the seaside/yard operation and the port energy system management within one unified framework by harnessing the synergy between two of the most prominent maritime electrification techniques: onshore power supply and microgrid. We formulate the joint scheduling problem as a two-stage model. In the first stage, the port authority determines the optimal berth allocation for the incoming vessels considering their cargo volumes, energy demands, and the availability of OPS facility and cargo handling equipment (i.e., quay/yard cranes). In the second stage, acting as the port microgrid operator, the port authority determines the optimal day-ahead scheduling of the container handling activities and operation of port microgrid assets for each time slot. Uncertainty from renewable energy generation and port load forecast is also incorporated in the problem formulation. The simulation-based case study shows that the proposed joint scheduling algorithm is capable of enhancing energy independence, system-wide efficiency, operational reliability, and economy of the port microgrid in comparison with the conventional berth allocation strategy. We hope our work provides insights into how electrification can help the maritime sector reinforce its commitment to sustainability while remaining competitive.

1. Introduction

As the backbone of a trillion-dollar maritime industry that moves 90% of the cross-border world trade as measured by volume, maritime ports are playing a pivotal role in advancing global trade and economies. However, these ports are also major sources of vessel-related air pollution [1,2]. When a vessel is docked to the port, its main propulsion engine is shut down. However, its auxiliary engine(s) remains on to supply the vessel's electric power demand for in-port activities such as cargo handling, lighting, heating, hot water, and ventilation. These operations consume a large amount of low-quality fuel such as marine diesel, gas oil, and heavy fuel oil, and account for a series of harmful environmental impacts including exhaust fumes, noise, vibrations, and air emissions (e.g., carbon (CO/CO_2), sulfur oxides (SO_x), nitrogen oxide (NO_x) and particulate matter (PM)) to the port workers, on-board personnel, and the port area communities and residents [3,4]. According to the estimate [5], nearly 70% of PM emissions from shipping (between 0.9 and 1.7 million tons) occur within 250 miles of the coast. Particularly in cases where ports are located near large metropolitan

* Corresponding author.
E-mail address: jshi14@uh.edu (J. Shi).

https://doi.org/10.1016/j.apenergy.2022.118856
Received 31 December 2021; Received in revised form 14 February 2022; Accepted 25 February 2022

Nomenclature

Sets

D	Set of berths, i= {1…, ND}, where ND is the number of berths.
K	Set of vessels, k = {1…, NK}, where NK is the number of vessels.
V	Set of quay cranes (QCs), v= {1…, NV}, where NV is the number of QCs.
C	Set of yard cranes (YCs), c= {1…, NC}, where NC is the number of YCs.
M	Set of energy storage systems, m={1…, NM}, where NM is the number of energy storage systems equipped in the port microgrid.
R	Set of renewable energy generators, r={1…, NR}, NR is the number of renewable energy generators in the port microgrid.
G	Set of dispatchable distributed generators (DGs), j= {1…, ND}, ND is the number of dispatchable DGs in the port microgrid.
T	Set of time segments, t={1…, 23}
S	Total number of scenarios.

Variables

$b_{j,t}$	1, if dispatchable unit j is on at time t; 0, otherwise.
λ_k/d_k	Actual arrival/departure time for vessel k.
$a_{i,k}$	1, if vessel k is assigned to berth i; 0, otherwise.
$st_{k,t}$	1, if vessel k starts berthing at time t; 0, otherwise.
$y_{i,k,t}$	1, if berth i is occupied by vessel k at time t; 0, otherwise.
$r_{k,t,v}$	1, if QC v is allocated to serve vessel k at time t; 0, otherwise.
$w_{k,t,c}$	1, if YC c are allocated to serve vessel k at time t; 0, otherwise.
$q_{j,t}$	Power output of dispatchable DG j attime t.
$x_{j,t}/z_{j,t}$	Startup/Shutdown indicator of DG j at time t.
q_t^c	Utility output to microgrid at time t.
$q_{m,t}^e$	Power output of energy storage m at time t.
$l_{s,t}^{sh}$	Load shedding amount at time t in scenario s.
$q_{s,t}^{cu}$	Amount of power curtailment at time t in scenario s.
$u_{m,t}$	1, if energy storage system m is discharging at time t; 0, otherwise.
$v_{m,t}$	1, if energy storage system m is charging at time t; 0, otherwise.
$C_{m,t}$	Stored energy in m at time t.

Parameters

EA_k/ED_k	Estimated arrival/departure time for vessel k.
c_1/c_2	Penalty cost of vessel k for berthing after EA_k/beyond ED_k.
E_k^{ves}	Energy consumption of vessel k at berth
E_k^{qc}/E_k^{yc}	Energy consumption of QCs/YCs allocated to vessel k at berth.
TA_k	Container amount of vessel k (TEU).
θ_1/θ_2	Handling efficiency of QCs/ YCs at each berth (TEU/h).
θ_k^Q/θ_k^C	The number of QCs/YCs allocated to vessel k at berth.
ζ_i^{ops}	OPS capacity installed at berth i.
Q_{qc}/Q_{yc}	Load rating of a QC/ YC per container move.
$X_{j,t}^{off/on}$	Off/on time of DG j at time t.
$T_j^{off/on}$	Minimum off/on time of DG j.
$Q^{c,min/max}$	Min/max power output from the utility at the PCC.
$Q_j^{min/max}$	Min/max power output of dispatchable DG j.
$P_{m,t}^{ch/dch,min/max}$	Min/max charge/discharge rate for energy storage m.
c_j	Operation cost for dispatchable DG j.
SU_j/SD_j	Shut-down/startup cost of dispatchableDG j.
ρ_t^c	Power price in the utility market.
α	Percentage of the shiftable vessel power demand.
E_k^s/E_k^f	Shiftable/Fixed energy consumption associated with vessel k at berth.
$q_{k,t}^{v,f,d}/q_{k,t}^{v,s,d}$	Fixed/Shiftable power demand of vessel k berthing at time t.
$q_{k,t}^{qc,d}/q_{k,t}^{yc,d}$	Shiftable power demand of QCs/YCs assigned to vessel k at time t.
$q_{k,t}^{s,d}/q_{k,t}^{f,d}$	Shiftable/Fixed power demand of vessel k at time t.
$\Delta q_{r,t,s}^{re}$	Renewable energy forecast deviation at time t in scenario s.
$\Delta q_{t,s}^{l}$	Load shedding forecast deviation at time t in scenario s.
H	A large positive number.
$VOLL$	Value of load shedding.
$VOPC$	Value of power curtailment.
ρ_t^c	Power price in the utility market.
α	Percentage of the shiftable vessel power demand.
E_k^s/E_k^f	Shiftable/Fixed energy consumption associated with vessel k at berth.

Acronyms/abbreviations

OPS	Onshore power supply
CBQ	Conventional berth-QC approach
DER	Distributed energy resource
BAP	Berth allocation problem
QC	Quay crane
YC	Yard crane

areas, ship emissions could often be one of the dominant sources of degraded air quality and urban pollution [6]. Based on the estimation of the European Federation for Transport and Environment, air pollution from international shipping results in approximately 50,000 premature deaths per year in Europe [7].

One of the most effective ways towards emission reduction for ships at berth is to use cold ironing. Cold Ironing, also known as shore-to-ship power supply or onshore power supply (OPS), allows a ship to be "plugged" into the port electricity system and utilize shore-side power supply from the port to support its energy demand while at berth [3,4]. In this way, a ship can completely shut down its auxiliary diesel-burning engine and utilize the onshore electricity, a much cleaner alternative to support its energy demand at berth without disruption to onboard services. In addition to drastically reducing harmful air emissions at the maritime ports, OPS can also eliminate the noise and small particle pollution in the port vicinity [8]. Numerous studies have shown that there are great environmental benefits of using the OPS. While the specific benefits of OPS are dependent on factors such as regional characteristics, grid conditions, and traffic patterns at ports, a previous study [9] has shown that, in the UK, implementing OPS would reduce the emissions of CO_2, SO_2, CO, and NO_x by 25%, 46%, 76%, and 92%, respectively, when compared with using marine diesel oil. According to the U.S. environmental protection agency (EPA), the benefits of OPS deployment contribute to 60%-80% reductions of emissions of CO_2 and other air pollutants from ships at different ports in America, Europe, and Asia [10].

The concept of "microgrid" is another emerging technological advance that has gained significant attention from the maritime industry in recent years [11–14]. A microgrid is a relatively small-scale localized energy network featuring an effective integration of high penetration

levels of distributed energy resources (DERs), such as renewable energy resources, energy storage devices, and controllable loads [15]. A microgrid can operate autonomously both in an island mode (i.e., disconnected from the main utility grid) or a grid-connected mode. With the recent trend of electrification of cargo handling equipment and the energy replacement of diesel to electricity, a microgrid is an emerging alternative to provide secure, high-quality, and green energy, which opens up opportunities for energy assurance, capacity expansion, sustainability enhancement, and operation continuity to further improve the port's smartness [11,16].

Despite the apparent benefits, the management of such a complicated maritime energy system, as shown in Fig. 1, is a complex optimization problem. Conventionally, the seaside operation includes the assignment of berth space and service time to vessels for loading/unloading operations, which is commonly referred to as the berth allocation problem (BAP) [19,20]. Meanwhile, the *trans*-shipment of cargo requires the coordination of port equipment such as quay cranes (QCs), yard equipment such as yard cranes (YCs), and cargo handling equipment [21]. The overall terminal operation can thus be modeled as an integrated logistic problem to focus on maximizing the operation efficiency and throughput of a port, leading to higher revenues. However, with the incorporation of OPS and given the significant vessel energy demand on the MW level, it is clear that the electrical characteristics of vessels have to be considered in the operation and management of the port energy system based on microgrid as well [22]. This is especially important to be considered together with the shoreside renewable generation, which can be a major source of uncertainties due to their highly volatile and stochastic nature. Hence, it is apparent that effective co-operation of berth allocation and port microgrid becomes crucial for fostering a resourceful, reliable, cost-effective, and sustainable marine energy system to mitigate emissions from shipping sectors, which are estimated to increase by 50 to 250% by 2050 [3].

To tackle this challenge, this paper proposes a novel joint scheduling algorithm to bridge the technological gaps in the conventional port scheduling paradigm and advance the energy system design and operation for maritime ports. We formulate the optimal day-ahead scheduling problem as a two-stage model. In the first stage, the port operator determines the optimal berthing time and position for the arriving vessels in the scheduling horizon to load and unload containers as a berth allocation problem (BAP). Then, the optimal scheduling of the port microgrid incorporating the OPS facility and container handling equipment is addressed in the second stage to optimize the port's energy and economic performance. The contributions of this paper can be summarized as follows:.

(1) This paper seeks the synergy between two of the most prominent maritime electrification techniques, OPS (as well as the associated berth allocation problem) and port microgrid, to expand the conventional scheduling practice of the port operation and enable an energy-efficient and environmentally friendly port.
(2) This paper presents a novel two-stage day-ahead scheduling strategy to jointly optimize the seaside/yard operations and port microgrid energy management. The proposed scheduling strategy enhances the service level of a port, as well as the reliability and efficiency of the port energy system, via an integrated approach. To the best of our knowledge, this paper is the first of its kind in this direction.
(3) This paper conducts a comprehensive study to highlight how the proposed scheduling approach can effectively harness the OPS and microgrid technology to improve the performance of a maritime port in terms of operation efficiency, electricity cost, emission mitigation, and energy independence.

The remainder of this paper is organized as follows. Section II describes the outlines, key structures, and assumptions of the proposed work. Section III formulates a two-stage stochastic programming model and the associated solution algorithm. The simulation-based case studies are presented in Section IV with the conclusions drawn in Section V.

2. Outline

2.1. Current research and industrial practice

Currently, there are many existing and ongoing efforts in the maritime industry to integrate microgrids into their energy system design. In the United States, in response to California's electrification push, the state's largest ports including Ports of San Diego (SD), Log Angeles (LA), and Long Beach (LB) are turning to microgrids for their superior efficiency and environmental footprints. The microgrid at Port of SD, anticipated to be installed starting early 2021, will consist of 700 kW of solar, 700 kW of energy storage as well as electric charging and shore power infrastructure to serve its Tenth Avenue Marine Terminal [23]. It is expected to save the port approximately 60% on electrical bills at the terminal per year. During an emergency such as a power outage, the microgrid is designed to maintain the operation of critical terminal infrastructure for approximately four hours. The microgrid will benefit the nearby San Diego International Airport and U.S. Navy base as well [24]. The Port of LA microgrid will incorporate a 1-MW solar PV array, an onshore 2.6-MWh battery storage system, and an updated electrical infrastructure to support the needs of heavy-duty electric trucks, yard tractors, and high-power electric vehicle chargers at its Green Omni Terminal [25,26]. During power outages, the microgrid will be able to island from the utility grid and meet the energy demand of the 40-acre facility. The project is anticipated to reduce 3,200 tons of greenhouse gases and nearly 28 tons of diesel PM, NO_x, and other harmful emissions from port operations annually [26]. The $7.1 million microgrid for Port of LB is anticipated to include a 300-kW solar array, a 330-kW stationary

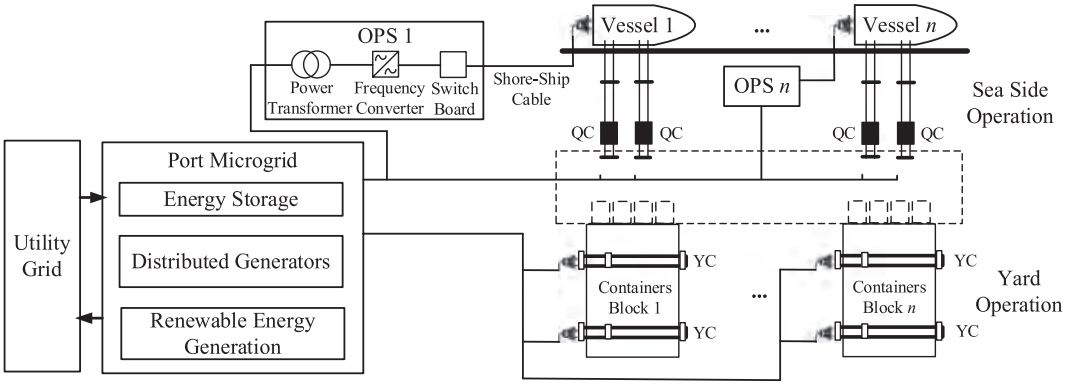

Fig. 1. Operation of a fully electrified port.

battery storage, a 250-kW mobile battery storage, and a 500-kW diesel generator [26,27]. The microgrid will facilitate the port's effort to become a zero-emission green port. It is also expected to increase the security, stability, and resiliency of the port's energy system. The commissioning of the Port LB microgrid is scheduled for August 2021 [27].

For European ports, many have invested in the infrastructure for renewable energy such as wind (e.g., 200 MW/45 MW/28.2 MW in ports of Rotterdam, Antwerp, and Amsterdam, respectively), solar panels (11GWh/750MWh/55MWh in the Ports of Amsterdam, Rotterdam, and Gothenburg, respectively), and wave/tidal energy [14]. Furthermore, the microgrid solution has been adopted by ports of Antwerp and Barcelona to effectively manage locally produced renewable energy [28,29]. Port of Rotterdam is also looking into the development of a virtual power plant (VPP) to integrate thermal and renewable energy resources [30]. The proposed VPP is expected to work as a microgrid cluster to enable emission reduction, demand-side management, and eventually increase the energy efficiency at the port. A block-chain-based trading platform is currently being evaluated to facilitate power transactions within the VPP [30].

2.2. Synergy between the OPS and port microgrid

The synergy between the OPS and a port microgrid can be enumerated in the following aspects:.

(1) Emission control: While OPS eliminates a large portion of environmental impacts produced by the ships at berth, the port microgrid provides the platform to further advance the port's sustainable initiatives and ultimately achieve the zero-net energy goal by utilizing low-carbon generation and renewable energy sources such as zero-/low-emission liquefied natural gas (LNG) and liquefied petroleum gas (LPG) powered engines, onshore and off-shore wind generation, solar generation, tidal energy, and on-site bioenergy [17,18]. Hence, the zero-emission combination of port microgrid and OPS provides true environmentally responsible energy and promotes the role of maritime transportation in answering the worldwide call to combat climate change and address the port's negative impact on the environment and public health.

(2) Energy efficiency and economics: Considering the ever-increasing traffic volume of vessels coming in and out of a port, the energy consumption from OPS poses significant challenges to the efficient and reliable operation of the onshore power system. A port microgrid, equipped with advanced operation and control techniques, provides a well-rounded solution to this challenge [31,32]. The multiple energy assets owned by the port microgrid and its intelligence allows it to optimally shift the combinations of renewable generation, storage, dispatchable units, and grid assets to provide the most cost-effective means of supply power. The advanced underlying smart grid technologies allow the port to be constantly operated in an efficient and economical way to intelligently dispatch the energy storage, reduce peak-hour demand, lower operation cost, and mitigate peak-hour costs while meeting the power demand and power quality requirements from the OPS facility and other port demands. Furthermore, a microgrid also ensures the seamless integration of the OPS and the shore power system where a complex power converter-based interfacing is required.

(3) Security and resiliency: OPS requires a continuous, high-quality power supply during the vessel's stay. Hence, a port with significant OPS installations can be vulnerable to power disturbances and outages. In this regard, a port microgrid equipped with local distributed generation and energy storage resources can operate in an island mode when the reliability of the utility grid deteriorates and thus adds significant power safety and security to the port and its OPS facility. This energy independence is particularly valuable in the face of weather-related extreme events, which occur more frequently with higher severity in recent years.

2.3. Joint berth and microgrid scheduling

In this paper, we propose a novel two-stage decision making process as shown in Fig. 2 to support the joint operation of the microgrid and OPS for vessels at berth. In the first stage, the port authority gathers information such as the anticipated arrival/departure schedule of a vessel and the total volume of containers to be loaded/unloaded from the vessel to estimate its total energy demand while at berth. Berth information will also be collected such as the berth status and the installed OPS power capacity. Based on the aforementioned information, the port authority can determine the optimal berth allocation considering the OPS allocation that minimizes the overall cost for the berthing of a vessel.

In the second stage, the port authority is acting as the port microgrid operator and determines the optimal day-ahead scheduling of the port microgrid assets considering the uncertainties from renewable energy sources and islanding situations. As a profit-driven entity, the objective of the port authority is to minimize the microgrid operation cost by effectively utilizing available local generation resources and energy storage systems, managing the load power consumption resulting from the port activities, and handling the interaction with the utility grid. The port authority also needs to perform load shedding and generation curtailment to maintain efficient and reliable port operation if the power balance of the port microgrid is disturbed.

The following assumptions are made in this article: During the berth scheduling stage, 1) the quay consists of a discrete number of berths and for each time segment of one hour, only one vessel can be served at every single berth; 2) there are no special constraints at the berth, which suggests no restriction regarding the ship length and draught; and 3) the scheduling horizon is divided into an equal time segment. For microgrid scheduling, the internal network of the port microgrid is not considered due to its limited geographical span. We consider two categories of DGs in the system: dispatchable DGs such as diesel/natural gas generators, and non-dispatchable units such as wind turbines and solar PV panels [11,17,28].

3. Model and method

We propose a two-stage model with the berth allocation problem in the first stage, followed by the port microgrid optimal scheduling problem in the second stage.

3.1. Berth allocation problem

Given the berth layout of a port and a set of vessels expected to be

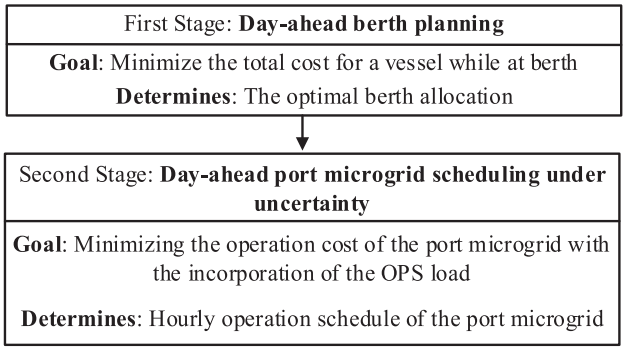

Fig. 2. Jointly optimized berth and microgrid scheduling.

served within the next 24 h scheduling horizon, the objective function of the BAP is to minimize the penalty cost representing the deviation between the service starting time and the expected arrival time, as well as the penalty cost caused by the deviation between the service finishing time and the expected departure time for all vessels as shown in (1):.

$$min\left\{\sum_k c_1(\lambda_k - EA_k)^+ + c_2\sum_k (ED_k - d_k)^+\right\} \quad (1)$$

The first and second terms of (1) are the summation of the costs associated with waiting time and delayed departure time of vessels, respectively. As the expected arrival time of the vessel is an agreement between the port and the shipping company, we consider vessels arriving at the port ahead of time would disrupt the subsequent berth allocation and the punctual departure of other vessels; hence is prohibited. Therefore, the first term only accounts towards the objective function when it is positive. Meanwhile, all vessels are expected to leave the port once the loading/unloading operation is completed. If a vessel needs to spend longer at the port than the expected departure time, it needs to pay a late departure penalty. However, no penalty applies if a vessel departs earlier than its scheduled departure time. This penalty is described in the second term of (1).

In (1), $(\lambda_k - EA_k)^+$ can be linearized by introducing a non-negative variable $x_{p,k}$ to replace $(\lambda_k - EA_k)^+$, and adding $x_{p,k} \geq \lambda_k - EA_k$ as a constraint. Similarly, $(ED_k - d_k)^+$ can be linearized by introducing a non-negative variable $x_{m,k}$ to replace $(ED_k - d_k)^+$. Then, the modified objective function can be expressed as:.

$$min\sum_k (c_1 x_{p,k} + c_2 x_{m,k}) \quad (2)$$

The constraints of the first stage model are defined in (2)-(16). Specifically, constraint (3) indicates that the actual arrival time of the vessel cannot be earlier than the expected arrival time of the vessel, to ensure the loading and unloading operation:.

$$\lambda_k \geqslant EA_k, \forall k \quad (3)$$

Constraint (4) entails that the handling capacity of each berth needs to be sufficient for a vessel to complete its loading and unloading operation. The handling capacity of each berth is measured by the maximum number of containers that can be handled at the berth per hour. The higher the handling capacity, the shorter the vessel has to stay at the port, which improves the operational efficiency and throughput of the port.

$$\sum_i \theta_1 \theta_k^Q a_{i,k} \geqslant TA_k \quad \forall k \quad (4)$$

Similarly, the capacity of the OPS installed on a specific berth should be sufficient to satisfy the vessel's energy demand from the onboard energy activities during the berthing time segments as depicted in (5):.

$$\sum_t \zeta_i^{ops} y_{i,k,t} \geqslant E_k^{ves} \quad \forall k, \forall i \quad (5)$$

Constraint (6) indicates that each vessel can have one and only one start time $st_{k,t}$ during the scheduling horizon. Hence, once the operation starts, the loading and unloading process lasts until it is completed.

$$\sum_t st_{k,t} = 1 \quad \forall k \quad (6)$$

Constraint (7) defines the actual departure time λ_k and describes the relationship between the actual arrival time and the actual departure time of a vessel.

$$\lambda_k = d_k + \sum_t \sum_i y_{i,k,t} - 1 \quad \forall k \quad (7)$$

Constraint (8) ensures that each berth can only serve one vessel at each time segment within the scheduling horizon. This constraint eliminates the potential space conflict among vessels per time segment.

$$\sum_k y_{i,k,t} \leqslant 1 \quad \forall i, \forall t \quad (8)$$

Constraint (9) ensures that each vessel can only be assigned to one berth. Constraint (10) denotes the relationship between $a_{i,k}$ and $y_{i,k,t}$.

$$\sum_i a_{i,k} = 1 \quad \forall k \quad (9)$$

$$\sum_t y_{i,k,t} - t \cdot a_{i,k} \leqslant 0 \quad \forall k, \forall i \quad (10)$$

Constraint (11) states that a vessel cannot change its position once it is berthed, i.e., no changing of berth is allowed during service.

$$d_k + H(y_{i,k,t} - 1) \leqslant t \cdot y_{i,k,t} \leqslant \lambda_k \quad \forall k, \forall i, \forall t \quad (11)$$

Upon the completion of the berth scheduling in the first stage, the total energy consumption of each ship and the QCs and YCs allocated to the ship is determined.

3.2. Port microgrid scheduling problem

The second stage problem is a microgrid scheduling problem, the objective function of which is to minimize the operation cost as shown in (12). This cost includes: 1) the operation cost of the microgrid's dispatchable DGs to produce energy, 2) the transaction cost between the port microgrid and the utility grid in the form of energy at the point of common coupling (PCC), and 3) the penalty cost associated with load shedding and power curtailment [33].

$$\begin{aligned} min &\sum_j \sum_t (c_j q_{j,t} + x_{j,t} SU_j + z_{j,t} SD_j) + \sum_t \left(\rho_t^c q_t^c\right) \\ &+ \frac{1}{N}\sum_{n=1}^{N}\left(\sum_s \sum_t (VOPC \cdot l_{s,t}^{sh} + VOLL \cdot q_{s,t}^{cu})\right) \end{aligned} \quad (12)$$

As a general rule of thumb, all the dispatchable DG units within the microgrid are subject to power capacity constraints (13) such that the maximum/minimum output of each generator is constrained. The dispatchable DG units are also subject to minimum uptime and downtime limitations as described in (14) and (15). Furthermore, the generator output is constrained by the ramp-up/down limits, as depicted in (16) and (17), respectively.

$$b_{j,t} Q_j^{g,min} \leqslant q_{j,t} \leqslant b_{j,t} Q_j^{g,max} \quad \forall j, \forall t \quad (13)$$

$$(X_{j,t}^{on} - T_j^{on})(b_{j,t-1} - b_{j,t}) \geqslant 0 \quad \forall j, \forall t \quad (14)$$

$$(X_{j,t-1}^{off} - T_j^{off})(b_{j,t} - b_{j,t-1}) \geqslant 0 \quad \forall j, \forall t \quad (15)$$

$$q_{j,t} - q_{j,t-1} \leqslant (2 - b_{j,t-1} - b_{j,t}) Q_j^{g,min} \quad \forall j, \forall t \quad (16)$$

$$q_{j,t-1} - q_{j,t} \leqslant (2 - b_{j,t-1} - b_{j,t}) Q_j^{g,min} \quad \forall j, \forall t \quad (17)$$

We consider the interaction between the port microgrid and the regional distribution system (i.e., the utility grid) involving the bi-directional exchange of energy (i.e., active power). Considering the physical limit of a PCC, we include the bounds for the energy interaction as shown in (18). Note that the default transfer direction is from the utility to the port microgrid; hence, a negative exchange indicates the port microgrid is selling surplus energy generated by its internal resources back to the utility.

$$Q^{c,min} \leqslant q_t^c \leqslant Q^{c,max} \quad \forall t \quad (18)$$

The port microgrid is equipped with energy storage systems. Each energy storage system can either be charged or discharged subject to its charging/discharging rate as described in (19) and (20). The charging/discharge state defined in (21) indicates that only one working mode is allowed at each time segment. The operation of the energy storage

system includes the bound of the variations of the state of charge (SoC) for each time segment, and the maximum/minimum state of charge allowed for reliable operation of the energy storage system as shown in (22) and (23):.

$$q^{e}_{m,t} \leqslant P^{dch,max}_{m,t} u_{m,t} - P^{ch,min}_{m,t} v_{m,t} \quad \forall m, \forall t \tag{19}$$

$$q^{e}_{m,t} \geqslant P^{dch,min}_{m,t} u_{m,t} - P^{ch,max}_{m,t} v_{m,t} \quad \forall m, \forall t \tag{20}$$

$$u_{m,t} + v_{m,t} \leqslant 1 \quad \forall m, \forall t \tag{21}$$

$$C_{m,t} = C_{m,t-1} - q^{e}_{m,t} \quad \forall m, \forall t \tag{22}$$

$$C^{min}_{m} \leqslant C_{m,t} \leqslant C^{max}_{m} \quad \forall m, \forall t \tag{23}$$

The power consumption within the port microgrid involves two parts: the port load and the load resulting from the vessel berthing and the associated cargo loading/unloading. While the total energy consumption associated with each vessel E_k is determined during its entire stay, the specific hourly power usage can be adjusted. More specifically, we assume that there is a certain percentage of E_k, namelyE^{f}_{k}, to support the essential hourly vessel operations while at berth, such as the air-conditioning, lighting, and hotel load, and thus is fixed as described in (25). The rest of the vessel energy consumption plus the energy consumption from the QC and YC operation to support the cargo transfer of vessel k is considered shiftable and can be adjusted by the microgrid operator during the vessel's berth as in (26). In this way, the port microgrid operator can schedule the handling of the vessels based on the operation status of the port microgrid in a flexible manner.

$$E_k = E^{s}_{k} + E^{f}_{k} \quad \forall k \tag{24}$$

$$E^{f}_{k} = (1-\alpha) E^{ves}_{k} \quad \forall k \tag{25}$$

$$E^{s}_{k} = \alpha E^{ves}_{k} + E^{qc}_{k} + E^{yc}_{k} \quad \forall k \tag{26}$$

Therefore, the fixed hourly load during a vessel's stay can be described as:.

$$q^{v,f,d}_{k,t} = E^{f}_{k} / (\lambda_k - d_k) \quad \forall k, \forall t \tag{27}$$

Meanwhile, the shiftable hourly load associated with each vessel is described in (28), which includes three terms: 1) the first term describes the vessel's load at berth; 2) the second term is the power demand from the QCs allocated for each vessel; 3) the last term is the power demand from the YCs allocated for each vessel:.

$$q^{s,d}_{k,t} = q^{v,s,d}_{k,t} + q^{qc,d}_{k,t} + q^{yc,d}_{k,t} \quad \forall k, \forall t \tag{28}$$

$$\sum_{t} q^{v,s,d}_{k,t} = \alpha E^{ves}_{k} \quad \forall k \tag{29}$$

$$\sum_{t} q^{qc,d}_{k,t} = E^{qc}_{k} \quad \forall k \tag{30}$$

$$\sum_{t} q^{yc,d}_{k,t} = E^{yc}_{k} \quad \forall k \tag{31}$$

The total power demand of QCs/YCs for each vessel is obtained by multiplying the number of QCs/YCs with their individual load rating and handling efficiency as shown in (32)-(33), respectively.

$$q^{qc,d}_{k,t} = \sum_{v} \theta_1 v r_{k,t,v} Q_{qc} \quad \forall k \tag{32}$$

$$q^{yc,d}_{k,t} = \sum_{c} \theta_2 c w_{k,t,c} Q_{yc} \quad \forall k \tag{33}$$

Constraints (34) and (35) ensure that the sum of the number of QCs/YCs allocated to each time segment is equal to the total number of QCs/YCs assigned to each vessel.

$$\sum_{t}\sum_{v} v r_{k,t,v} = \theta^{Q}_{k} \quad \forall k \tag{34}$$

$$\sum_{t}\sum_{c} c w_{k,t,c} = \theta^{C}_{k} \quad \forall k \tag{35}$$

In the handling process of vessels, the assignment of QCs and YCs should be properly synchronized. Constraint (36) assures that QCs are assigned to each vessel at berth. On the other hand, (37) indicates the link that the allocated QCs and YCs should be active simultaneously to transport the containers:.

$$\sum_{v} r_{k,t,v} = \sum_{i} y_{i,k,t} \quad \forall k, \forall t \tag{36}$$

$$\sum_{v} r_{k,t,v} = \sum_{c} w_{k,t,c} \quad \forall k, \forall t \tag{37}$$

It is noted that the hourly vessel load cannot exceed the maximum capacity of each OPS:.

$$q^{v,f,d}_{k,t} + q^{v,s,d}_{k,t} \leqslant \sum_{i} \zeta^{ops}_{i} a_{i,k} \quad \forall k, \forall t \tag{38}$$

The shiftable energy will be used to handle power curtailment and load shedding caused by the errors from the output forecast of renewable energy and load as follows:.

$$\sum_{r} \Delta q^{re}_{r,t,s} + l^{sh}_{s,t} = \Delta q^{l}_{t,s} + q^{v,s,d}_{k,t,s} + q^{qc,d}_{k,t,s} + q^{yc,d}_{k,t,s} + q^{cu}_{s,t} \quad \forall k, \forall t, \forall s \tag{39}$$

The load shedding and power curtailment will be included in the objective function of microgrid scheduling. Meanwhile, the microgrid power balance needs to be ensured, such that the power imported from/exported to the utility, storage system, dispatchable generator, and renewable generator should be equal to port microgrid load plus load related to vessel berthing, which includes the power consumption of the vessels at berth and the quay/yard equipment, including QC loads and YC loads. The power balance is captured by constraint (40):.

$$q^{c}_{t} + \sum_{m} q^{e}_{m,t} + \sum_{j} q_{j,t} + \sum_{r} q^{re}_{r,t} = q^{l}_{t} + \sum_{k} q^{v,f,d}_{k,t} + \sum_{k} q^{s,d}_{k,t} \quad \forall t \tag{40}$$

3.3. Uncertainty modeling

Two major sources of uncertainty considered in this paper are renewable energy generations and load consumption in the microgrid. For the purpose of scheduling, the forecasted values will be used with a normal distribution to describe the forecasting error. The probability distributions of the renewable energy output and hourly load forecast are defined in (41) and (42), respectively:.

$$q^{re}_{r,t} \sim N(\overline{W}_t, \sigma^{2}_{r,t}) \forall r, \forall t \tag{41}$$

$$q^{l}_{t} \sim N(\overline{L}_{l,t}, \sigma^{2}_{l,t}) \ \forall l, \forall t \tag{42}$$

The mean values of the normal distribution are the forecasted hourly load consumption and renewable energy generation, and the standard deviation is set to be 10% of the expected hourly values, respectively.

4. Numerical experiments

We evaluate the performance of the proposed approach through a set of simulation-based case studies consisting of a terminal with five berths equipped with OPS. The specification of OPS installation and the energy usage profile of the terminal are modified based on the actual information of the fourth phase of Yangshan Port in Shanghai, China [34]. More specifically, the capacity of the OPS installation at each berth is shown in Table 1. We assume that each berth can allow up to 4 QCs to

Table 1
Berth Information.

Berth #	OPS capacity (MW)	Maximum number of deployable QCs for each berth
1	1	4
2	1	4
3	1.5	4
4	1.5	4
5	2	4

operate simultaneously. To avoid potential congestion, the terminal can allow up to 12 QCs and 20 YCs to operate simultaneously. The detailed information of the vessel fleet including their arrival, due time, auxiliary engine rating, and cargo to be handled is modified from [21], which is also based on Yangshan Port, and provided in Table 2.

For the port energy system, we consider a microgrid with five dispatchable DG units, two non-dispatchable (i.e., renewable) DG units (one wind generator and one solar generator), and one energy storage system. The detailed specifications are adopted from [11] which discusses the sizing of port microgrid and are provided in Table 3 and 4, respectively.

To evaluate the environmental impacts of the port and vessel operation, the following emission coefficients as shown in Table 5 are adopted for the pollutants of CO_2, SO_2, NO_x, PM_{10}, and $PM_{2.5}$ for the marine diesel fuel and the dispatchable generating units within the port microgrid, respectively. Note that the emission coefficients for marine diesel fuel used in the case study were taken from literature [35] and [36]. These parameters are also consistent with the "Fourth IMO Greenhouse Gas Study 2020" conducted by the International Maritime Organization (IMO) [37]. Meanwhile, the emission coefficients for the Dispatchable DGs (micro-turbines) were adopted from the latest "Emission Factors for Greenhouse Gas Inventories" recommended by the U.S. Environmental Protection Agency [38]. We assume that all the dispatchable units are micro-turbines equipped with standardized air pollution control devices.

The following simulation results were obtained using GAMS [39] on a laptop equipped with 1.60 GHz Intel© CPU and 8 GB of RAM.

4.1. Performance evaluation

We first evaluate the performance of the proposed approach compared to a benchmark that adopts the conventional berth-QC (hereinafter referred to as CBQ) scheduling [19–41]. CBQ model has been commonly adopted in the literature to study the optimal port operation scheduling with both BAP and conventional port energy system scheduling taken into account. More specially, the goal of the CBQ scheduling is to minimize the total operating cost of vessels while at

Table 2
Vessel Information.

Vessel name	Arrival time	Due time	Container (TEU)	Required vessel power at berth (MW)	QCs required	YCs required
MSG	9	15	428	1.99	13	18
NTD	10	16	455	0.7	13	19
CG	3	8	259	0.7	8	11
NT	20	24	172	0.32	6	7
LZ	12	20	684	1.26	20	28
XY	4	10	356	0.7	11	15
LZI	8	14	435	0.7	13	18
GC	11	16	350	0.43	10	14
LP	19	23	150	0.32	5	6
LYQ	18	23	400	0.83	12	16
CCG	10	15	333	0.63	10	14

Table 3
Characteristics of dg units. (D: Dispatchable, ND: Non-Dispatchable).

DG Unit	Type	Cost Coefficient ($/MWh)	Min.-Max. capacity (MW)
G1	D	21.6	4–15
G2	D	33.8	2.5–12
G3	D	45.4	2–10
G4	D	52.8	1.5–8
G5	D	66.3	0.8–5
G6	ND	0	0–4
G7	ND	0	0–5

Table 4
Characteristics of the energy storage system.

Storage	Capacity (MWh)	Min.-Max. Charging/DischargingPower (MW)
ESS	20	0–5

Table 5
Emission coefficients of diesel (g/kg) and DG(g/mw).

	CO_2	SO_2	NO_x	PM_{10}	$PM_{2.5}$
Marine diesel fuel	3160	0.35	47.6	1.4	1.4
Dispatchable DGs (micro-turbines)	725	0.032	0.2	0.04	0

berth, which includes penalty cost for vessels not arriving and departing on time, OPS electricity cost, QC electricity cost, and YC electricity cost as shown in (43). Furthermore, it is assumed in the CBQ model that the port is not equipped with a microgrid and thus it has to purchase all the power from the utility grid. It is thus evident that CBQ takes into account the impact of the energy price fluctuations on the selection of berths and the operation status of cargo handling equipment. Similar to the proposed approach, the CBQ approach is subject to a set of operation-related and OPS-related constraints (1)-(11), (32)-(38), as well as (44) and (45).

$$min\left\{\sum_k c_1(\lambda_k - EA_k)^+ + \sum_k c_2(ED_k - d_k)^+ + \sum_k\sum_t \rho_t^c(q_{k,t}^v + q_{k,t}^{qc} + q_{k,t}^{yc})\right\} \tag{43}$$

s.t. (1)–(11), (36)–(37), and.

$$\sum_t q_{k,t}^v = E_k^{ves},\ \sum_t q_{k,t}^{qc} = E_k^{qc},\ \sum_t q_{k,t}^{yc} = E_k^{yc} \forall k \tag{44}$$

$$q_{k,t}^v \leqslant \sum_i \zeta_i^{ops} a_{i,k} \forall k, \forall t \tag{45}$$

The energy and operational performance comparisons of the proposed joint scheduling approach and CBQ are shown in Table 6. We can clearly observe that when OPS is fully integrated into the port energy system, the traditional CBQ scheduling suffers from a longer waiting time (5 h) than the proposed approach (1 h). The detailed berth allocations for both approaches are shown in Fig. 3. More specifically, Fig. 3 (a) shows that vessel GC experiences a three hour wait because CBQ is attempting to take advantage of the low electricity price and assign as many QCs as possible to existing vessels, which results in a QC shortage for new incoming vessels. Then, vessel LYQ also experiences a two hour wait as the time period of 17:00–20:00 is the peak of the electricity price, and CBQ chooses to delay the operation of vessel LYQ to avoid the excessive energy cost of QCs and YCs. By contract, we can see in Fig. 3(b) that vessel LZ only experiences a one hour wait as there are no idle QCs available at the port between 12:00 and 13:00 in the proposed approach. We can also observe that the operation of vessels is not affected during

Table 6
Comparison of CBQ and the proposed joint scheduling approach.

	Total handlingTime (h)	Waiting Time (h)	Total QC energy consumption (MWh)	Total QC energy cost ($)	Total YC energy consumption (MWh)	Total YC energy cost ($)	Total OPS energy consumption (MWh)	Total OPS energy cost ($)	Total port energy system operation cost ($)
CBQ	47	5	28.093	1851.069	17.288	1223.36	11.98	2908.32	6616.352
Proposed approach	43	1	28.093	1793.452	17.288	1082.32	9.96	2703.27	6404.475

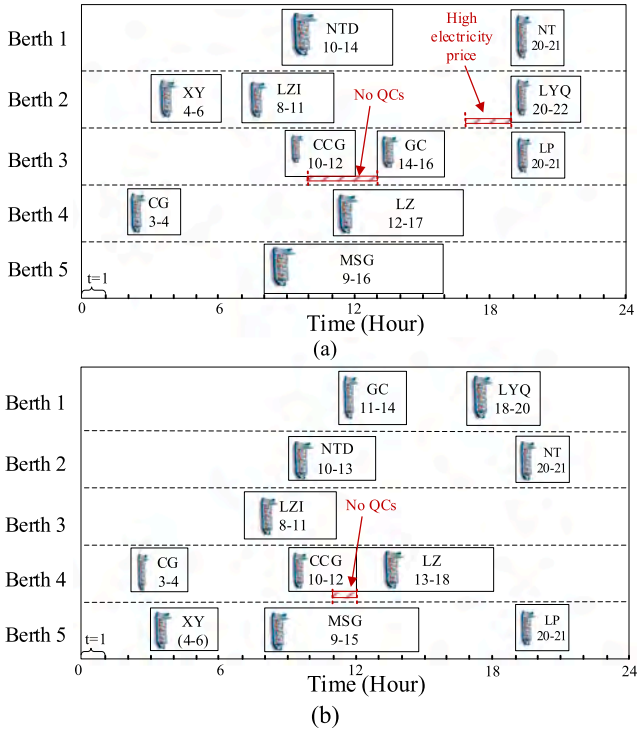

Fig. 3. The berth allocation for (a) the CBQ scheduling and (b) the proposed scheduling approaches.

the peak hours in the proposed approach, thanks to the support from the port microgrid.

Meanwhile, Table 6 indicates that the total port energy system operation cost for the proposed approach is 7.6% lower than CBQ. More specially, while the total energy consumption from QCs and YCs are identical for both approaches, their associated energy cost is roughly 3% and 13% lower for the proposed approach, respectively. This is because the proposed scheduling approach fully utilizes the renewable energy and energy storage integrated into the port microgrid, yielding a lower energy cost. For the OPS, we can observe that due to the shortened total berth time for vessels at the port, less energy is required to support the operation of the OPS facility, which yields a lower overall energy cost as well.

Furthermore, Fig. 4 depicts the detailed power generation profiles for CBQ and the proposed approach, respectively. It can be observed in Fig. 4 (a) that, under CBQ, since the port operator relies on the utility grid to satisfy the port's power demand, it has to continue importing energy when the market price is high between 16:00 and 20:00. By contrast, the proposed approach allows the port energy system to be operated in a more flexible and independent fashion. Fig. 4 (b) shows that when the electricity market price is low during the off-peak hours, the port operator tends to keep the DGs within the port microgrid shut down and import power from the utility grid. However, when the market price rises, the port operator starts to switch to the DGs and energy storage system within the port microgrid to meet the port's power demand. In particular, between 12:00 and 23:00, we can observe that the port is completely relying on the port microgrid for its energy demand. The port operator also continues to export the additional power generated by the port microgrid back to the utility grid during peak hours to alleviate the burden of the main grid and gain economic benefits.

Fig. 5 illustrates the detailed energy consumptions from different port equipment and facilities. It can be observed that for the 24-hour scheduling horizon, the operation of QCs consumes roughly half of the total energy demand of the port for both scheduling approaches. The YCs and OPS facilities, on the other hand, account for around 30% and 20% of the total energy consumption of the port. The energy consumption profile shows that QCs can be the main energy consumer in the port energy system. Therefore, improving the energy efficiency of the QCs through methods such as adjustments of configuration and operation procedures can be an effective way to reduce the port's overall energy consumption. This finding is consistent with the literature [42].

4.2. Impact of OPS capacity

Based on the previous discussion, it is apparent that the capacity of the OPS facility affects the berthing choices for vessels, and to a certain extent, has an impact on the operation of the port. In the following analysis, we consider six different OPS configurations to evaluate the impacts of OPS installations on the port operation in terms of operation efficiency and emission reduction based on the proposed joint sched-

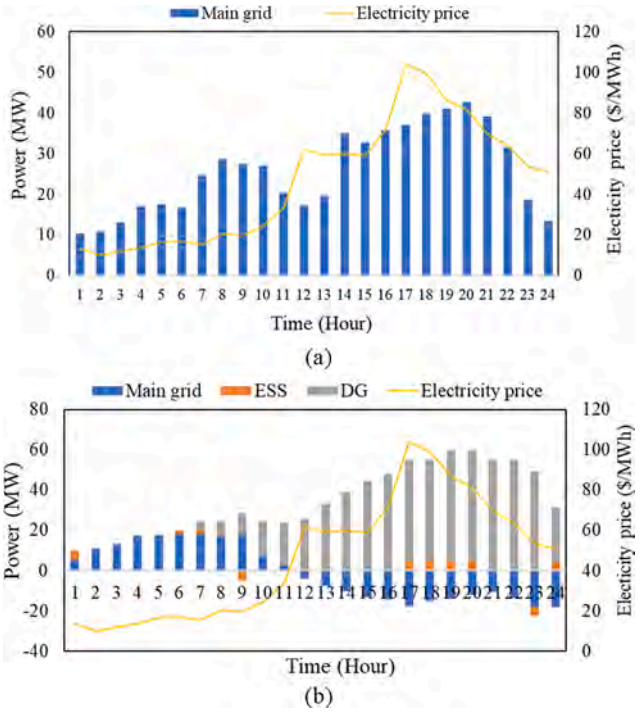

Fig. 5. Energy consumptions profiles for (a) CBQ and (b) the proposed scheduling approach.

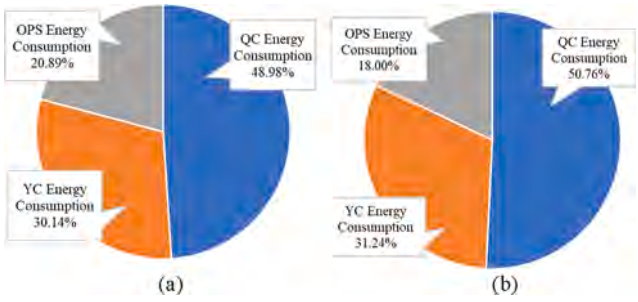

Fig. 4. Power generation profile for (a) CBQ and (b) the proposed approach.

uling approach. The results of this analysis are given in Table 7. Note that the emissions are calculated using the following equation [21]:.

$$EM_i = l^A(P_i^A R_i^A)t_i^{berth}\omega_c \quad (46)$$

where ω_c is the emission coefficient for different pollutants, P_i^A denotes the auxiliary engine's power rating for vessel i, R_i^A denotes the auxiliary engine's fuel consumption rate, l^A denotes the engine's load coefficient. In the following analysis, l^A is set to 0.5 and R_i^A is set to 0.211 kg/kWh for all vessels [35].

Table 7 indicates that when there are no OPS installed (i.e., Case 1), the overall handling time is 42 h. Since no OPS is installed at the berth, the vessels have to use their onboard auxiliary engines using marine diesel fuel, which results in large amounts of greenhouse gas and air pollutants, such as CO_2, SO_2, NO_x, and PMs. When the terminal is partially covered with OPS as in cases 2 and 3, we can observe that the total handling time slightly increases (from 42 h to 43/44 h) as the berthing allocation needs to take the shoreside OPS capacity and vessel power demand at berth into account. Since some berths are not equipped with the OPS facility, the port operator has to delay the operations of certain vessels to assure the vessels can depart on time and sufficiently utilize the OPS resource while at berth. Meanwhile, it is clear to see that the emissions start to decrease as the power demands of vessels are being met by the shoreside electricity. More specifically, the CO_2, SO_2, NO_x, PM_{10}, and $PM_{2.5}$ pollutants are lowered by roughly 43%, 26%, 7%, 21%, and 21%, respectively. This improvement demonstrates the effect of OPS on emission reduction.

When we further increase the coverage of OPS in Case 4 and Case 5 to the extent that every berth is equipped with an OPS facility, it can be observed that the total handling time remains at 43/44 h. Due to the increased use of OPS, the emissions significantly declined. Compared to Case 1, the CO_2, SO_2, NO_x, PM_{10}, and $PM_{2.5}$ pollutants are lowered by roughly 85%, 94%, 99%, 99%, and 100%, respectively. This shows that when a terminal is fully covered with OPS, the greenhouse emissions and toxic air pollutants can be significantly curbed, and some are eliminated. In Case 6, we consider the case where all the berths are equipped with OPS facilities of the maximum capacity (2 MW) that can satisfy the individual power demand of all incoming vessels. While such a case could be potentially expensive for the port entity to install and maintain, we can observe that it offers the best operation efficiency and emission reduction. The total handling time is 42 h, suggesting that as all the berths are covered with the maximum OPS capacity, the berth allocation is no longer constrained by the compatibility of shoreside and onboard power ratings, assuring the operation efficiency. Meanwhile, similar to Case 4 and Case 5, Case 6 provides excellent emissions reduction.

Finally, we analyze the energy consumption as well as the costs associated with the OPS facility. Table 7 shows that as the coverage of OPS increases, the energy consumption also increases. Note that the OPS energy consumption in Case 6 is lower than in Case 4 and Case 5, which can be attributed to the shortened total handling time. When the vessels spend less time at berth, it is reasonable to expect a decreased OPS consumption. We can observe a similar trend for the OPS operation cost: when more berths are equipped with OPS installations, more electrical energy is consumed, leading to a higher operation cost.

Based on the above analysis, it is evident that from the scheduling perspective, installing sufficient capacity OPS facilities at all berths could effectively curb the emissions level for a terminal without interfering with the vessels' cargo handling operations. However, this may represent significant investment challenges to the port entity due to the large capital cost associated with the high-capacity OPS facility deployment.

5. Conclusions and Future work

This paper presented a novel two-stage day-ahead scheduling approach to jointly optimize the terminal operation and port microgrid energy management in the context of the ever-increasing electrification of port energy infrastructure. The proposed approach enables the port operator to decide the berthing time, berthing location, and quay/yard equipment assignment for the arriving vessels in the first stage. In the second stage, the port operator determines the optimal scheduling of the port microgrid with the incorporation of OPS to optimize the port's energy performance. Simulation results highlight the advantages of the proposed approach compared to the conventional terminal operation scheduling strategy that entirely relies on the utility grid. More specifically, we have shown that the proposed scheduling approach is capable of harnessing the latest OPS and microgrid technology for improved operation efficiency, lowered electricity bills, significantly reduced emissions, and complete energy independence. Furthermore, we have analyzed the impacts of OPS capacity and coverage rate on the scheduling performance. Simulation results have shown that a port can operate more effectively when all the berths are equipped with OPS facilities with sufficiently large capacities. Our work is one of the pioneering efforts to show that smart energy technologies can be deployed in the maritime environment to advance the operation of maritime transportation systems. We hope the presented research provides insights into how electrification can help the maritime sector and other traditional energy-intensive and heavily polluting industries reinforce their commitment to sustainability while remaining competitive.

Future studies can extend the research presented in this manuscript to evaluate the most cost-effective configuration of the port microgrid to support the incorporation of OPS. Furthermore, one can also study the optimal voyage planning, with the joint operation of port microgrid and OPS taken into account, to determine the fastest and most economically

Table 7
Impacts of OPS installation.

	OPS capacity (MW)	Total handling time (h)	OPS energy consumption (MWh)	OPS operation cost ($)	CO_2 (kg)	SO_2 (kg)	NO_x (kg)	PM_{10} (kg)	$PM_{2.5}$ (kg)
Case 1	0/0/0/0/0	42	0	0	2860.4	0.31	43.087	1.267	1.267
Case 2	0/0/1/1.5/2	43	6.12	1603.27	1624.82	0.23	39.433	1.004	0.984
Case 3	0/0/2/2/2	44	6.23	1613.17	1637.38	0.24	40.002	1.007	1.097
Case 4	1/1/1/1.5/2	44	10.16	2763.562	479.224	0.0244	0.158	0.00448	0
Case 5	1/1/1.5/1.5/2	43	9.96	2703.27	448.251	0.0229	0.136	0.00418	0
Case 6	2/2/2/2/2	42	9.82	2693.27	423.635	0.0206	0.112	0.00377	0

viable route from the port of origin to the destination.

CRediT authorship contribution statement

Yue Zhang: Conceptualization, Methodology, Software, Formal analysis, Investigation, Writing – original draft, Writing – review & editing. **Chengji Liang:** Conceptualization, Validation, Investigation, Resources, Supervision. **Jian Shi:** Conceptualization, Methodology, Investigation, Formal analysis, Writing – original draft, Writing – review & editing. **Gino Lim:** Conceptualization, Investigation, Writing – review & editing, Resources, Supervision. **Yiwei Wu:** Methodology, Software, Validation, Investigation.

Declaration of Competing Interest

The authors declare the following financial interests/personal relationships which may be considered as potential competing interests: This work was supported by the Soft Science Research Project of Shanghai Science and Technology Innovation Action Plan (No. 22692111200), the National Key Research and Development Plan of China (No. 2019YFB1704403), and the National Natural Science Foundation of China (No. 71972128).

References

[1] Sornn-Friese H, Poulsen RT, Nowinska AU, de Langen P. What drives ports around the world to adopt air emissions abatement measures? Transport Res Part D Transport Environ 2021;90:102644. https://doi.org/10.1016/j.trd.2020.102644.
[2] Cammin P, Yu J, Heilig L, Voß S. Monitoring of air emissions in maritime ports. Transport Res Part D Transport Environ 2020;87:102479. https://doi.org/10.1016/j.trd.2020.102479.
[3] Zis TPV. Prospects of cold ironing as an emissions reduction option. Transportation Research Part A: Policy and Practice 2019;119:82–95.
[4] Dai L, Hu H, Wang Z, Shi Y, Ding W. An environmental and techno-economic analysis of shore side electricity. Transport Res Part D Transport Environ 2019;75:223–35.
[5] O. Merk, " Shipping Emissions in Ports,". *International Transport Forum*, [Online] Available at: https://www.itf-oecd.org/sites/default/files/docs/dp201420.pdf (accessed July 2021).
[6] Sciberras EA, Zahawi B, Atkinson DJ. Reducing shipboard emissions – Assessment of the role of electrical technologies. Transport Res Part D Transport Environ 2017;51:227–39.
[7] Winkel R, Weddige U, Johnsen D, Hoen V, Papaefthimiou S. Shore side electricity in Europe: potential and environmental benefits. Energy Policy 2016;88:584–93.
[8] IMO, 2018. "Shore Power," *International Maritime Organization (IMO), London.* [Online] Available at: http://glomeep.imo.org/technology/shore-power (accessed July 2020).
[9] Hall WJ. Assessment of CO2 and priority pollutant reduction by installation of shoreside power. Resour Conserv Recycl 2010;54(7):462–7.
[10] United States Environemtnal Agency, "Shore power technology assessment at U.S. ports," March, 2017.
[11] Molavi A, Shi J, Wu Y, Lim GJ. Enabling smart ports through the integration of microgrids : A two-stage stochastic programming approach. Appl Energy 2020;258:114022.
[12] Fang S, et al. Towards future green maritime transportation: an overview of seaport microgrids and all-electric ships. IEEE Trans Veh Technol 2020;69:207–19.
[13] Ahamad NB, Guerrero JM, Su C, Vasquez JC, Zhaoxia X. Microgrids technologies in future seaports. In: 2018 IEEE International Conference on Environment and Electrical Engineering and 2018 IEEE Industrial and Commercial Power Systems Europe (EEEIC / I&CPS Europe); 2018. p. 1–6.
[14] Roy A, Auger F, Olivier J-C, Schaeffer E, Auvity B. Design, sizing, and energy management of microgrids in harbor areas: a review. Energies 2020;13(20):5314. https://doi.org/10.3390/en13205314.
[15] Hatziargyriou N, Asano H, Iravani R, Marnay C. Microgrids. IEEE Power Energy Mag 2007;5(4):78–94.
[16] Wang L, Liang C, Shi J, Molavi A, Lim G, Zhang Y. A bilevel hybrid economic approach for optimal deployment of onshore power supply in maritime ports. Appl Energy 2021;292:116892. https://doi.org/10.1016/j.apenergy.2021.116892.
[17] Molavi A, Lim GJ, Shi J. Stimulating sustainable energy at maritime ports by hybrid economic incentives: A bilevel optimization approach. Appl Energy 2020;272:115188. https://doi.org/10.1016/j.apenergy.2020.115188.
[18] Gutierrez-Romero JE, Esteve-Pérez J, Zamora B. Implementing onshore power supply from renewable energy sources for requirements of ships at berth. Appl Energy 2019;255:113883.
[19] Bierwirth C, Meisel F. A survey of berth allocation and quay crane scheduling problems in container terminals. Eur J Oper Res 2010;202(3):615–27.
[20] Chang D, Jiang Z, Yan W, He J. Integrating berth allocation and quay crane assignments. Transport Res Part E Logist Transport Rev 2010;46(6):975–90.
[21] Liang C, Huang Y, Yang Y. A quay crane dynamic scheduling problem by hybrid evolutionary algorithm for berth allocation planning. Comput Ind Eng 2009;56(3):1021–8.
[22] Innes A, Monios J. Identifying the unique challenges of installing cold ironing at small and medium ports – The case of Aberdeen. Transport Res Part D Transport Environ 2018;62:298–313.
[23] Port of San Diego, "Energy & Sustainability," [Online] Available at: https://www.portofsandiego.org/environment/energy-sustainability/energy (accessed July 2021).
[24] L. Cohn, "Port of San Diego to demonstrate how microgrids benefit ports worldwide," [Online] Available at: https://microgridknowledge.com/microgrids-benefit-ports-san-diego/ (accessed July 2021).
[25] A. Burger, "Port of Los Angeles microgrid project nears finish line," [Online] Available at: https://microgridknowledge.com/microgrid-port-of-los-angeles/ (accessed July 2021).
[26] J. Gerdes, "California ports turn to microgrids for energy security, demand flexibility," [Online] Available at: https://www.greentechmedia.com/articles/read/california-ports-turning-to-microgrids-for-energy-security-demand-flexibility (accessed July 2021).
[27] Port of Long Beach, "Port of Long Beach microgrid - resilience for critical facilities," [Online] Available at: https://californiaseec.org/wp-content/uploads/2019/07/Fact-Sheet-Port-of-Long-Beach-Microgrid.pdf (accessed July 2021).
[28] Rolán A, Manteca P, Oktar R, Siano P. Integration of cold ironing and renewable sources in the Barcelona smart port. IEEE Trans Ind Appl 2019;55(6):7198–206.
[29] J. Jones, "Port of Antwerp to lead energy innovations in European ports," [Online] Available at: https://www.smart-energy.com/industry-sectors/smart-energy/port-of-antwerp-to-lead-energy-innovations-in-european-ports/ (accessed July 2021).
[30] J. Jones, "Blockchain-powered microgrid pilots renewables trading in Port of Rotterdam," [Online] Available at: https://www.renewableenergyworld.com/storage/blockchain-powered-microgrid-pilots-renewables-trading-in-port-of-rotterdam/ (accessed July 2021).
[31] Sadiq M, et al. Future Greener Seaports: A Review of New Infrastructure, Challenges, and Energy Efficiency Measures. IEEE Access 2021;9:75568–87.
[32] Mutarraf MU, et al. A Communication-Less Multimode Control Approach for Adaptive Power Sharing in Ship-Based Seaport Microgrid. IEEE Trans Transp Electrif Dec. 2021;7(4):3070–82.
[33] Khodaei A. Resiliency-oriented microgrid optimal scheduling. IEEE Trans Smart Grid 2014;5(4):1584–91.
[34] Shanghai International Port Group, "Sustainability Report 2020," Available at: https://www.portshanghai.com.cn/xxpl/index.jhtml.
[35] Peng Y, Li X, Wang W, Liu Ke, Bing X, Song X. A Method for Determining the Required Power Capacity of an On-Shore Power System Considering Uncertainties of Arriving Ships. Sustainability 2018;10(12):4524. https://doi.org/10.3390/su10124524.
[36] Peng Y, Li X, Wang W, Wei Z, Bing X, Song X. A Method for determining the allocation strategy of on-shore power supply from a green container terminal perspective. Ocean Coast Manag 2019;167:158–75.
[37] International Maritime Organization (IMO), "Fourth IMO Greenhouse Gas Study 2020", [Online] Available at: https://www.imo.org/en/OurWork/Environment/Pages/Fourth-IMO-Greenhouse-Gas-Study-2020.aspx (accessed July 2021).
[38] U.S. Environmental Protection Agency, "Emission Factors for Greenhouse Gas Inventories," [Online] Available at: https://www.epa.gov/sites/default/files/2021-04/documents/emission-factors_apr2021.pdf.
[39] Rosenthal RE. "GAMS: A Users Guide," 2016. GAMS Development Corporation, Washington, DC, USA.
[40] Xiang X, Liu C, Miao L. Reactive strategy for discrete berth allocation and quay crane assignment problems under uncertainty. Comput Ind Eng 2018;126:196–216.
[41] Tan C, He J. "Integrated proactive and reactive strategies for sustainable berth allocation and quay crane assignment under uncertainty", *Ann.* Oper Res 2021.
[42] Iris Ç, Lam J. Optimal energy management and operations planning in seaports with smart grid while harnessing renewable energy under uncertainty. Omega 2021;103.